Fracture 1977, Volume 3, ICF4, Waterloo, Canada, June 19 - 24, 1977

STRESS CORROSION CHARACTERISTICS OF TOUGHENED GLASSES AND CERAMICS

J. T. Hagan, M. V. Swain and J. E. Field*

INTRODUCTION

The full potential of glasses and ceramics is being exploited by various toughening techniques, whereby high compressive stresses are induced chemically or thermally in the surface regions of these materials. These biaxial compressive stresses have to be overcome before fracture will occur. It has been shown by Kirchner and Walker [1] that the stress corrosion characteristics of toughened and untoughened alumina are the same and that the effect of the toughening is to provide sufficient strength at stress levels where failure usually occurs in untreated samples. Hagan and Swain [2] have made similar observations on chemically toughened calcium alumino silicate.

Attempts at using data from time to failure under static load or unnotched dynamic fatigue tests (Evans and Wiederhorn [3]) give anomalously high values of the stress corrosion index $\underline{n}$ for the toughened materials. Clearly the fracture stresses have to be corrected for the residual compressive stresses induced by the toughening. It is also apparent that the high tensile stresses in the middle of the toughened glasses or ceramics will have a significant effect on the times to failure, especially at stress levels not high enough to cause immediate failure. These internal stresses make it impossible to determine the stable sub-critical crack growth rates. It is however still possible to obtain the stress corrosion characteristics from the usual time to failure or dynamic fatigue data as suggested by Evans and Wiederhorn [3]. The analysis presented here is a simple modification of Evans' treatment for untoughened materials. This analysis rationalizes the proper corrections to be applied to the stresses and the effect of the high tensile stress, in the central region, arising from the toughening.

ANALYSIS

For both physically and chemically toughened glasses, the requirement for equilibrium is that the summation of the forces through the thickness, d, of the material must be zero;

$$\int_0^d \sigma\,(x)\,dx = 0 \qquad (1)$$

For thermally toughened glasses, the stress distribution throughout the thickness is parabolic (Zijlstra and Burggraaf [4]). The maximum compressive stress on the outer surfaces (x = 0, and x = d) is $-\sigma_c$. Consideration of equation (1) and the boundary conditions leads to

*Cavendish Laboratory, Cambridge, England.

$$\sigma_t = -\sigma_c \left(1 - \frac{6x}{d} + \frac{6x^2}{d^2}\right) \tag{2}$$

where the compression zone on either surface is ∿ 20% of the plate thickness, and the maximum central tensile stress at x = d/2 is $\sigma_c/2$ as suggested by Zijlstra and Burggraaf. The stress distribution in a bar arising from flexure (four point bend test) is of the form

$$\sigma_\beta = \sigma_\beta^* \left(1 - \frac{2x}{d}\right) \tag{3}$$

where σ_β^* is the stress in the outer fibre (at x = 0). For a thermally toughened bar under pure bending, the resultant stress distribution (residual toughening stress and bending stress) is

$$\sigma_\beta = \sigma_t + \sigma_\beta \tag{4}$$

Substituting for σ_t and σ_β for equations (2) and (3) respectively leads to

$$\sigma = \left(\sigma_\beta^* - \sigma_c\right) + \frac{x}{d}\left(6\sigma_c - 2\sigma_\beta^*\right) - \left(\frac{x}{d}\right)^2 6\sigma_c \tag{5}$$

This resultant stress σ for two values σ_β^*/σ_c is shown in Figure 1a.

For a straight (through-the-thickness) surface crack (with its origin at x = 0, and tip at x = c) in a single variable stress field of the form σ = σ(x), the stress intensity factor as given by Paris and Sih [5] is

$$K = 2Y\left(\frac{c}{\pi}\right)^{1/2} \int_0^c \frac{\sigma(x)\, dx}{\sqrt{c^2 - x^2}} \tag{6}$$

where Y is a dimensionless factor dependent on the crack shape, c is the final crack length and σ(x) is the stress function normal to the crack path.

This equation applies only for a crack in an infinite solid. For values of c << d (c ≲ .1d) this is a good approximation to the stress intensity factor for a semi-infinite solid in pure bending given by Brown and Srawley [6]. For larger values of c/d, a complete analysis needs to incorporate the interaction with the opposite boundary.

In the stress field defined by equation (5) the stress intensity factor is given by

$$K = Y\left(\sigma_\beta^* - \sigma_c\right)(\pi c)^{1/2}\left[1 + \frac{\alpha c}{d}\right] \tag{7}$$

where $\alpha = \frac{2}{\pi}\,\frac{6\sigma_c - 2\sigma_\beta^*}{\sigma_\beta^* - \sigma_c}$

Assuming a value of 60 MPa for the residual stress in a plate 5 mm thick and Y = 1 the stress intensity factors for four different values $\sigma_\beta^* = 0$, $\sigma_\beta^* = 1.5\,\sigma_c$, $\sigma_\beta^* = 2\,\sigma_c$ and $\sigma_\beta = 3\,\sigma_c$ are plotted in Figure 1b.

Knowing the stress intensity factor at the crack and a relationship between the crack velocity and the stress intensity factor driving the crack, one can obtain estimates of time to failure of components under the prescribed static stress. For most materials, it has been shown that the velocity and the stress intensity factor are related through

$$V = AK^n \tag{8}$$

where A and n are constants dependent on the material and the environment in which propagation occurs. The time to failure of the material under stress is

$$\tau = \int_{c_i}^{c_f} \frac{dc}{V} \tag{9a}$$

or

$$= \int_{c_i}^{c_f} \frac{dc}{AK^n} \tag{9b}$$

where c_i and c_f are the initial and final crack lengths respectively.

Substituting for the stress intensity given by equation (7) into (9b) and assuming Y = 1, the time to failure becomes

$$\tau = \int_{c_i}^{c_f} \frac{dc}{A\left(\sigma_\beta^* - \sigma_c\right)^n (\pi)^{n/2}\, c^{n/2}\left[1 + \frac{\alpha c}{d}\right]^n} \tag{10}$$

If $\left|\, \sigma c/d \,\right| < 1$, and n is large and the initial stress intensity factor $K < 0.9\, K_{Ic}$ (the critical stress intensity factor), then the time to failure τ is dominated by the initial flaw size c_i (Beaumont and Young [7]), and equation (10) after a binomial expansion and integration reduces to

$$\tau = \frac{2\, M(x_i)\, c_i^{\frac{2-n}{2}}}{A\left(\sigma_\beta^* - \sigma_c\right)^n (\pi)^{n/2}(n-2)} \tag{11}$$

where $M\left(x_i\right) \simeq 1 - n(n-2)\, x_i\, \frac{\alpha}{n-4}$

The dimensionless factor $M(x_i)$ may be regarded as a modifying term or magnification factor to the applied stress and becomes increasingly important as the normalized crack length $x_i = c/d$ increases to ∿.1.

It is now possible to rewrite equation (11) in a simplified form, as

$$\tau\left(\sigma_\beta^* - \sigma_c\right)^n = c_i = \text{constant} \tag{12}$$

Similarly it can be shown that for the dynamic fatigue test, the modified expression relating the fracture stress σ_β^* and the stress rate for either chemically or thermally toughened specimens is

$$\frac{(\sigma_\beta^* - \sigma_c)^{n+1}}{\dot{\sigma}} = c_i = \text{constant} \qquad (13)$$

where σ_c is the value of the residual stress in the outer fibre, $\dot{\sigma}$ is the stressing rate and α is a constant incorporating the crack propagation constants A, n and the ratio of failure stress, and K_{Ic} (see Evans and Johnson [8]).

RESULTS

Analysis of Kirchner and Walker's [1] data of Table 1, the time to failure for toughened and untoughened alumina shows that the stress corrosion index for untreated alumina in water is 23. For thermally toughened alumina in water, the stress corrosion index is 70, which is anomalously high. When the fracture stresses are corrected, for the toughening residual stresses, one obtains a value of ∿35. These values compare with the value of 31 obtained by Evans [9].

We have similarly obtained the stress corrosion index of 12 from time to failure data on Triplex Ten Twenty toughened soda lime glass. Allowing for the rather limited number of data points and the uncertainty in the value of the residual compressive stress, the value of $n \sim 12$ is in reasonable agreement with values of 14.1 and 16 obtained by Evans [8] and Wiederhorn and Bolz [10] for soda lime glass in water

Ritter and Cavanagh [11] have recently reported studies on the fatigue resistance of surface recrystallised lithium alumino silicate. By correcting for the residual stresses in the as-drawn specimens, they have obtained excellent agreement in the stress corrosion index for the as-drawn and annealed specimens.

The dynamic fatigue test has also been used to obtain the stress corrosion index for thermally toughened bars of alumino silicate in water. To obtain reproducible data (less than 5% scatter), to lower the fracture stress and to provide well-defined flaws from which fracture will initiate, controlled surface flaws were introduced, with Vickers microindentation, in the surface to be put in tension.

For the dynamic fatigue test, a load of 200 gm was used to induce flaws in all the specimens. The specimens in a water environment were loaded in four point bend jig with outer and inner spans of 100 mm and 50 mm respectively. Specimens were fractured at deflection rates of 10 mm/min down to 0.0097 mm/min. The stress corrosion index of 27 was obtained by least-square fit by minimizing the error in the fracture stress. This value compares with that of 25 for alumino silicate in water, obtained by Wiedernorn and Bolz [10]. Tests on annealed soda lime yielded a stress corrosion index of 18 (see Figure 2).

ACKNOWLEDGEMENT

This work was supported by the S.R.C. and the Procurement Executive, Ministry of Defence. The receipt of a preprint by B. R. Lawn and D. B. Marshall in the early stages of the work is gratefully acknowledged.

REFERENCES

1. KIRCHNER, H. P. and WALKER, R. E., Mat. Sci. and Eng. 8, 1971, 301.
2. HAGAN, J. T. and SWAIN, M. V., unpublished work 1976.
3. EVANS, A. G. and WIEDERHORN, S. M., Int. J. Fract. 10, 1974, 379.
4. ZIJLSTRA, A. L. and BURGGRAAF, A. J., J. Non-cryst. Solids 1, 1968, 49.
5. PARIS, P. C. and SIH, G. C., ASTM Spec. Tech. Publications 381, 1965, 30.
6. BROWN, W. F. and SRAWLEY, J. E., ASTM STP No. 410, 13.
7. BEAUMONT, W. R. and YOUNG, R. J., J. Mat. Sci. 10, 1975, 1334.
8. EVANS, A. G. and JOHNSON, H., J. Mater. Sci. 10, 1975, 214.
9. EVANS, A. G., J. Mater. Sci. 7, 1972, 1137.
10. WIEDERHORN, S. M. and BOLZ, L. H., J. Amer. Ceram. Soc. 52, 1970, 543.
11. RITTER, J. E. Jr. and CAVANAGH, M. S., J. Amer. Ceram. Soc. 59, 1976, 57.

Table 1 Data from Kirchner and Walker [1]

Time to failure s	Fracture Stress (psi)		
	A	B uncorrected	C corrected
1	50	100	50
10	47.1	98.5	48.5
10^2	44.1	94.8	44.8
10^3	41.54	92.3	42.3
10^4	38.46	89.2	39.23
10^5	36.9	86.2	36.2

A : untreated alumina in air

B : quenched alumina in water

C : quenched alumina in water (corrected for toughening residual stress)

1 psi = 6.89×10^3 Pa.

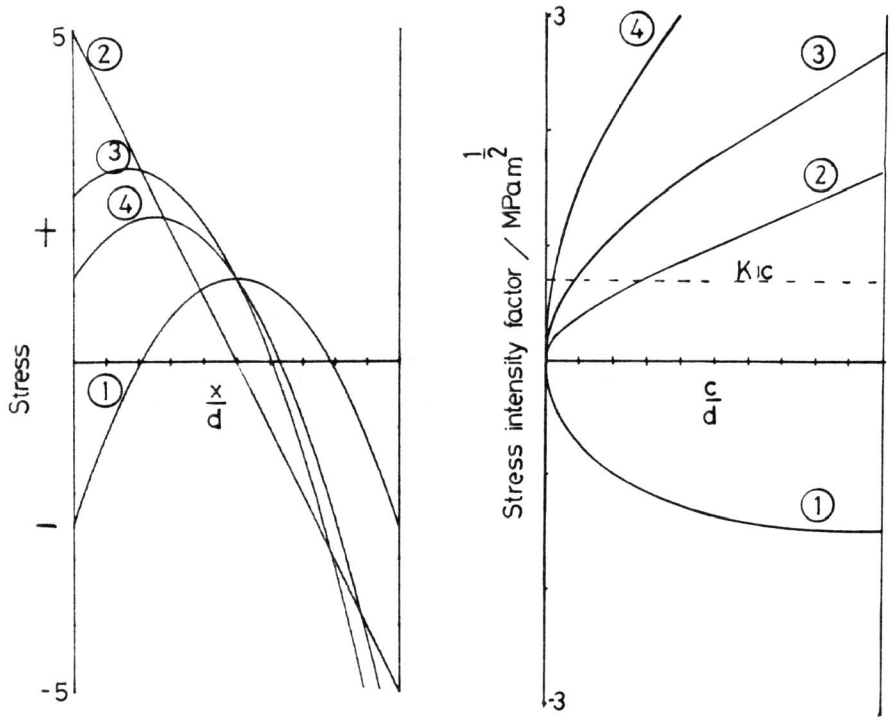

(a) (b)

Figure 1 (a) Stress Distribution in Plate. Curves (1) and (2) are the Residual Stress σ_c and Bending Stress σ_β, Respectively ($\sigma_\beta^* = 2\ \sigma_c$). The Resultant of These is Curve (3). Curve (4) is the Resultant Stress for $\sigma_\beta^* = 1.5\ \sigma_c$ ($\sigma_c = 2.5$ units)

(b) Stress Intensity Factor at Crack Tip in Plate 5 mm Thick for the Ratios of Applied Stress σ_β^* to Residual Stress σ_c of $\sigma_\beta^*/\sigma_c = 0$ (Curve (1)), 1.5 (Curve (2)), 2 (Curve (3)). $\sigma_c = 60$ MPa. Dotted Line is the Position of K_{Ic} for Soda Lime Glass

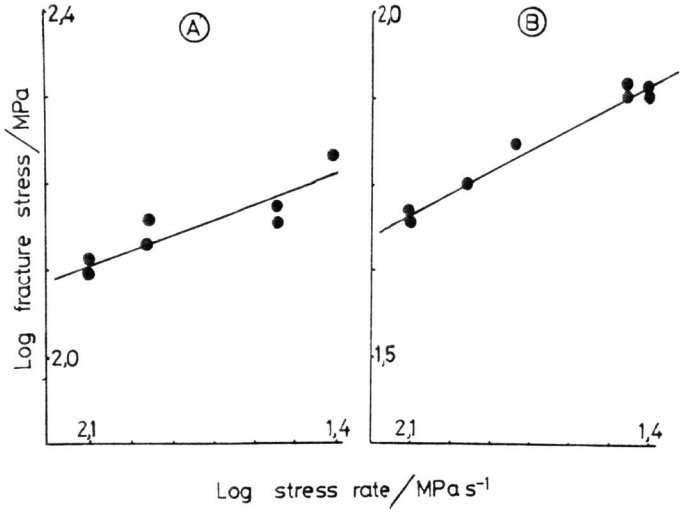

Figure 2 Dependence of the Fracture Stress on the Stress Rate for Toughened Alumino Silicate (A) and Annealed Soda Lime Glass (B)